Materials Research. 2015; 18(5): 939-945
DOI: http://dx.doi.org/10.1590/1516-1439.346614

One-step Synthesis of Ag_3PO_4/Ag Photocatalyst with Visible-light Photocatalytic Activity

Kai Huang[a], Yaohui Lv[a]*,Wei Zhang[a]*, Shanyun Sun[a],

Bin Yang[a], Fangli Chi[a], Songlin Ran[a], Xianguo Liu[a]

[a]School of Materials Science and Engineering, Anhui Key Laboratory of Metal Materials and Processing, Anhui University of Technology, 243002, Maanshan, Anhui, P. R. China

Received: November 6, 2014; Revised: May 17, 2015

A highly efficient photocatalyst Ag_3PO_4/Ag was prepared by a one-step low temperature chemical bath method. The reflectance spectra (DRS) indicated Ag_3PO_4/Ag had strong absorption in visible light region. The synthesized Ag_3PO_4/Ag photocatalyst was used as the efficient photocatalysts for the photocatalytic degradation of Rhodamine B (RhB) under visible-light illumination which showed almost complete degradation (~ 98%) of RhB dye in 90 min. The negative surface of Ag_3PO_4/Ag photocatalyst also promoted the degradation of a cationic dye like methylene bule (MB; 78% in 90min), while the performance against an anionic dye like methyl orange was poorer (MO; 40% in 90 min). Compared to the pure Ag3PO4 photocatalyst, the Ag_3PO_4/Ag photocatalyst showed the enhanced visible light photocatalytic informance. The excellent photocatalytic performance is mainly ascribed to the surface plasmon resonance of Ag nanoparticles and a large negative charge of PO_4^{3-} ions.

Keywords: *Ag_3PO_4/Ag, chemical synthesis, photocatalysis, visible light*

1. Introduction

Semiconductor-based photocatalysts have attracted considerable attention due to their potentially promising avenue for solving current environment and energy problems, by using the abundant solar light[1]. Of the well-known photocatalysts, titanium oxide (TiO_2) has undoubtedly proven to be the most promising material, due to its low toxicity, earth abundance, chemical and thermal stability, and resistance to photocorrosion[2]. Unfortunately, this commonly used photocatalyst, with a relatively wide band gap (3-3.2 eV), can only absorb a small fraction of solar energy (< 5%), which limits its practical applications. Therefore, development of more efficient photocatalysts is urgent and indispensable.

Recently, it has been demonstrated that plasmonic nanostructures of noble metals (mainly silver and gold) show significant promising in the field of photocatalysis[3]. A series of new hybrid photocatalysts on the basis of surface plasmon resonance (SPR) of metal nanoparticles[4,5], namely, plasmonic photocatalysts[6], were developed to decompose various organic pollutants under visible-light irradiation. Tobaldi et al.[7,8] have reported that the incorporation of Ag NPs can significantly improve the photocatalytic activity of TiO_2 nanopowders. Chen et al.[9] also revealed that the SPR effect of Au nanoparticles could induce visible-light-driven photocatalytic activity of Au/ZrO_2 and Au/SiO_2 photocatalyst. Ag/silver halide structure has been developed as a visible-light photocatalyst to enhance the photocatalytic activity of semiconductor, such as Ag/AgCl[10], Ag/AgBr[11] and Ag/AgI[12]. These catalysts displayed high photocatalytic activity and good stability under visible light due to the localized surface plasmon resonance (LSPR) effect of silver nanoparticles produced on the surface of silver halide.

Silver orthophosphate (Ag_3PO_4), a new type of photocatalyst reported by Ye et al.[13-15], has been demonstrated to show excellent photocatalytic ability for O_2 evolution from water as well as great photodecomposition of organic compounds. Interestingly, in order to promote the charge separation efficiency of the Ag_3PO_4 semiconductor, selective growth of Ag_3PO_4 submicron-cubes on Ag nanowires to construct necklace-like hetero-photocatalysts and two-dimensional dendritic Ag_3PO_4 nanostructures was demonstrated by this group[16,17]. The effect of particle size[18,19], pH value[20] and morphology[21,22] of silver phosphate on its photocatalytic activity have also been investigated. Unfortunately, one major limitation of this novel photocatalyst is the instability upon photo-illumination, since it is easily corroded by the photogenerated electrons (4Ag3PO4 + 6H2O + 12h+ + 12e- → 12Ag + 4H3PO4 + 3O2)[13]. Therefore, it is highly desirable to develop effective strategies to improve the stability of the Ag_3PO_4 photocatalyst. Recent reports indicated that AgX (X=Cl, Br, I) nanoshells on the surface of Ag_3PO_4 can enhance their photocatalytic properties and stability[23]. Furthermore, carbon quantum dots[24], graphene oxide[25,26], TiO_2[27], Bi_2MoO_6[28], SnO_2[29] and Fe_3O_4[30] were successfully used to form Ag_3PO_4 based hybrid nanostructures for getting enhanced photocatalytic activity and stability. The origin of photocatalytic performance of Ag_3PO_4 using first-principles density functional theory was investigated[31-33]. The excellent photocatalytic performance of Ag_3PO_4 is partly attributed to the highly dispersive band structure of the conduction-band minimum (CBM) resulting from Ag *s*-Ag *s* hybridization without localized *d* states.

*e-mail: yaohui@ahut.edu.cn, zw2010@ahut.edu.cn

Inspired by this study, Ag/Ag_3PO_4 was successfully synthesized as highly efficient and stable plasmonic photocatalyst[34-36]. However, most of the reported synthesis methods require surfactant, such as using pyridine, or in relatively complicated process. Here, we design a one-pot, simple experimental approach to prepare the Ag_3PO_4/Ag photocatalyst to improve the stability of Ag_3PO_4. The photocatalytic activity evaluation was carried out by decomposing methyl orange (MO), rhodamine (RhB) and methyl blue (MB) under visible irradiation at room temperature. Based on the experimental results, the photocatalytic reaction mechanism of the Ag_3PO_4/Ag plasmonic photocatalyst was discussed.

2. Experimental

2.1. Preparation of Ag_3PO_4/Ag photocatalyst

All the reagents used in this work were in analytical grade without further purification, and purchased from Shanghai Reagents Company (Shanghai, China). Bare Ag_3PO_4 powder samples were prepared by the simple ion-exchange method. In a typical synthesis, 0.018 mol $AgNO_3$ was dissolved in 100 mL of DI water. Na_2HPO_4 aqueous solution (0.12 M) was added drop by drop to the solution, under magnetic stirring, until the initial white colour changed to yellow. The resulting products were washed with DI water for several times, and finally dried at 70 °C for 5 h in a vacuum.

The Ag_3PO_4/Ag plasmonic photocatalysts were prepared by a one-step low temperature chemical bath method. In a typical synthetic route, 0.005 mol of silver nitrate ($AgNO_3$) was added to 50 ml ethylene glycol (EG) under vigorous stirring, and the resultant solution was marked as solution A. The solution which was marked as solution B results from the dissolution of $Na_2HPO_4 \cdot 12H_2O$ (0.001 mol) in 50 ml EG under vigorous stirring. When solutions A and B became clear, they were mixed together and stirred for 2 h until to assure homogeneity. The solution was heated in an oil bath at 160 °C for 30 min. The resulting precipitates were washed with DI and absolute ethanol several times and then dried at 70 °C for 5 h. A schematic diagram of the catalyst preparation process is shown in Figure 1.

2.2. Characterization of photocatalysts

The X-ray powder diffraction (XRD) patterns of the as-prepared catalysts were characterized by using a Bruker D8 advance powder X-ray diffractometer with Cu *K*α radiation (λ=1.54056 Å) in the 2θ range from 20° to 70°. Field-emission scanning electron microscope (FESEM, JEOL-6300F) was employed to characterize the morphologies and size of the synthesized samples. UV-vis diffuse reflectance spectra were obtained for the dry pressed disk samples by using a Shimadzu UV 2550 recording spectrophotometer, which was equipped with an integrating sphere, and $BaSO_4$ was used as a reference.

A Zeta potential analyzer, (Zetapals, Brookhaven Instruments Corporation, USA) was used to characterize the electrokinetic properties of the Ag_3PO_4/Ag photocatalysts. For the Zeta potential measurement, an Ag_3PO_4/Ag photocatalyst suspension of 2 mg/ml concentration was prepared by dispersing Ag_3PO_4/Ag powder in deionized water under continuous magnetic stirring. The effect of pH (in the range of 5-11) on the electrokinetic properties was investigated by measuring the zeta potential under distinct pH values, changed by using 0.1 M HNO_3 (in the acidic range) and 0.1 M (alkaline range) solutions.

2.3. Evaluation of photocatalytic performance

MO (anionic dye), MB and RhB (cationic dyes) were selected as model chemicals to evaluate the activity and properties of the Ag_3PO_4/Ag photocatalyst. A 300 W Xe arc lamp (PLS-SXE300, Beijing Trusttech Co., Ltd.) equipped with an ultraviolet cutoff filter to provide visible light was used as the light source. The distance between it and the photocatalyst was 50 cm. The light intensity reaching the samples was measured using a radiometer and was found to be approximately 35 W m^{-2} in the visible-light range. In a typical experiment, 250 ml aqueous suspensions of

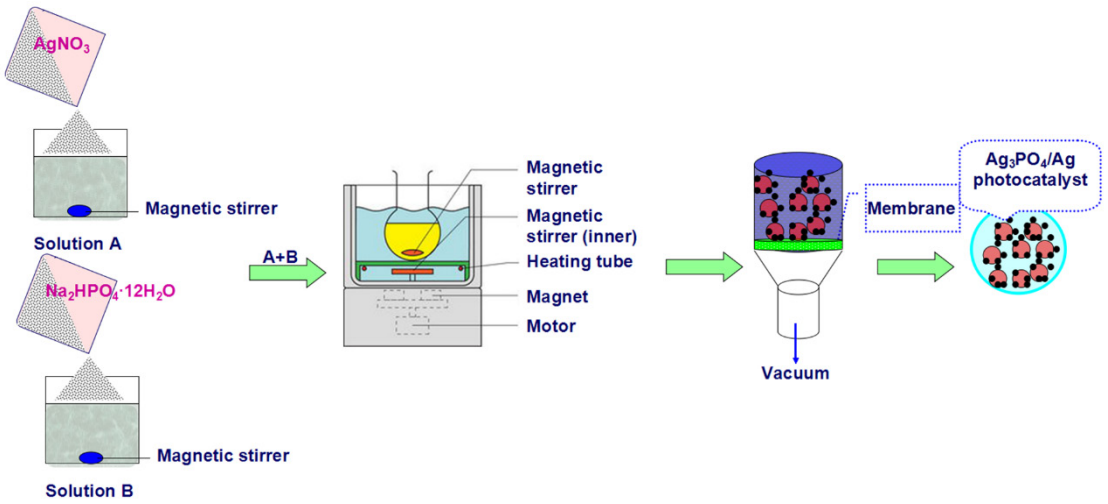

Figure 1. A schematic diagram of the preparation processof Ag_3PO_4/Ag photocatalyst.

RhB (10 mg/L) and 100 mg of photocatalyst powders were placed in a test tube. Prior to irradiation, the suspensions were magnetically stirred in the dark for 30 min to establish adsorption/desorption equilibrium between the dye and the surface of the catalyst under room air equilibrated conditions. At given irradiation time intervals, about 5 ml of the suspension was collected and centrifuged to remove the catalyst particulates for analysis. The residual dye absorption property was detected using a UV-vis spectrophotometer (Hitachi UV-3100)

3. Results and Discussions

The crystalline structure of the as-prepared sample has been examined, as shown in Figure 2. Figure 2a shows the typical powder X-ray diffraction (XRD) pattern of the product. It can be clearly seen that the diffraction peaks can be indexed to the pure body-centered cubic (bcc) structure of Ag_3PO_4 with cell constant of a= 6.013 Å (JCPDS no. 84-512). Figure 2b is a typical XRD pattern of the as-obtained Ag_3PO_4/Ag sample. All the diffraction peaks in this pattern can be categorized into two sets. The diffraction peaks that marked with "▼" can be readily indexed to cubic Ag_3PO_4 (JCPDS no. 84-512), while the peak labeled with "★" can be indexed to cubic phase Ag (JCPDS no. 87-717). No other crystalline impurities can be observed. The strong diffraction peaks of Ag indicate the good crystallinity degree of Ag in the Ag_3PO_4/Ag plasmonic photocatalyst.

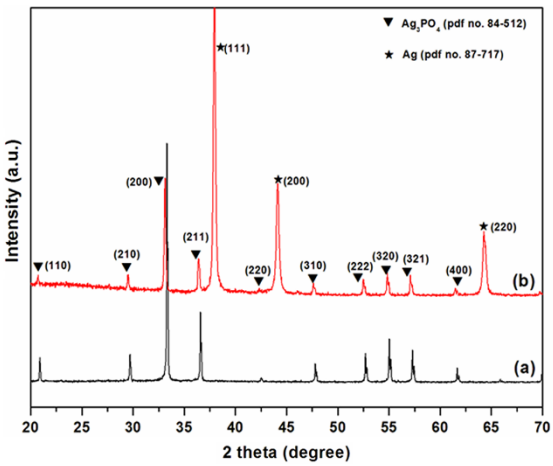

Figure 2. XRD patterns of the (a) Ag_3PO_4 photocatalyst and (b) Ag_3PO_4/Ag photocatalyst.

The morphology and size of the pure Ag_3PO_4 and the Ag_3PO_4/Ag were investigated with SEM and TEM techniques. Figure 3a depicts a typical SEM micrograph of the pure Ag_3PO_4 sample, revealing the spherical morphology with uniform size of about 800-900 nm. Figure 3b shows a SEM image of the prepared Ag_3PO_4/Ag photocatalyst. It can be seen that Ag_3PO_4/Ag photocatalyst is composed of many tiny spherical Ag_3PO_4 nanoparticles dispersed on the surface of the spherical Ag particles. Figure 3c shows the representative TEM micrographs of Ag_3PO_4/Ag photocatalyst. As shown in Figure 3c, the TEM image confirms that a large quantity of Ag_3PO_4 nanocrystals are attached onto the surface of the spherical Ag, and the size of Ag_3PO_4 nanoparticles is mostly in the range of 100-200 nm.

The UV-Vis diffuse reflectance spectra of as-prepared Ag_3PO_4 and Ag_3PO_4/Ag photocatalysts are shown in Figure 4. It is observed that pure Ag_3PO_4 could absorb visible light with a wavelength shorter than 530 nm (shown in Figure 4a), in agreement with the results previously reported[15]. However, for Ag_3PO_4/Ag plasmonic photocatalyst, except for a much higher absorbance than Ag_3PO_4 at the range of 500-800 nm, a new broad absorbance peak at 320 nm has been observed, which should be ascribed to the metallic Ag particles (shown in Figure 4b). Remarkable absorption enhancement in visible light region is beneficial for improving photocatalytic activity in this irradiation region.

The photocatalytic performances of Ag_3PO_4/Ag plasmonic photocatalyst and of pure Ag_3PO_4 particles for the RhB degradation have been studied and are compared in Figure 5. As shown in this figure, it can be clearly seen that the Ag/Ag_3PO_4 composite shows a higher photocatalytic activity for the decomposition of RhB compared with Ag_3PO_4 photocatalyst. Furthermore, the photocatalytic stability of Ag_3PO_4/Ag was investigated by recycling in the repeated RhB degradation experiments. As shown in Figure 6, the RhB dye is quickly bleached after every RhB decomposition experiments, and Ag_3PO_4/Ag photocatalysts are stable enough during the repeated experiments without exhibiting any significant loss of photocatalytic activity. Therefore, the as-prepared Ag_3PO_4/Ag composites can work as effective photocatalysts for organic compounds degradation with good

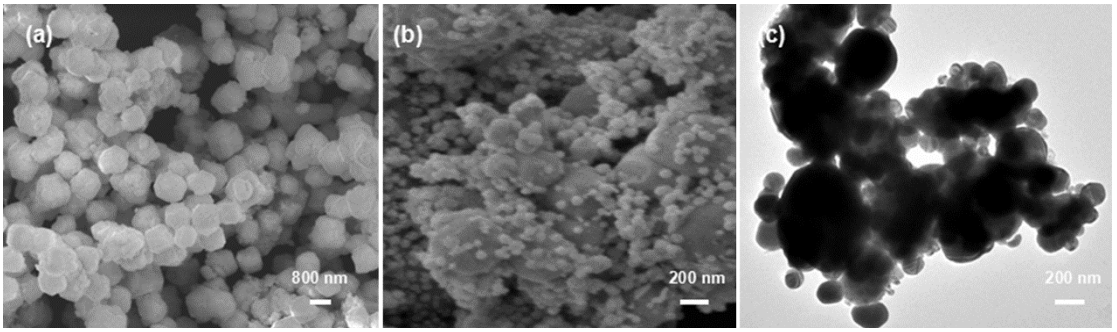

Figure 3. SEM images of (a) Ag_3PO_4, (b) Ag_3PO_4/Ag and TEM image of (c) of Ag_3PO_4/Ag photocatalyst.

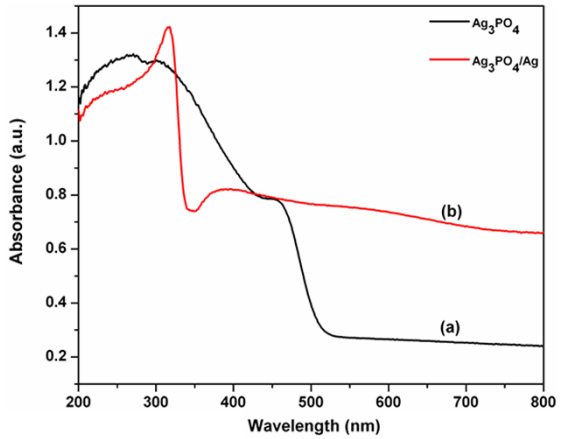

Figure 4. UV-vis absorption spectrum of (a) Ag_3PO_4 photocatalyst and (b) Ag_3PO_4/Ag photocatalyst.

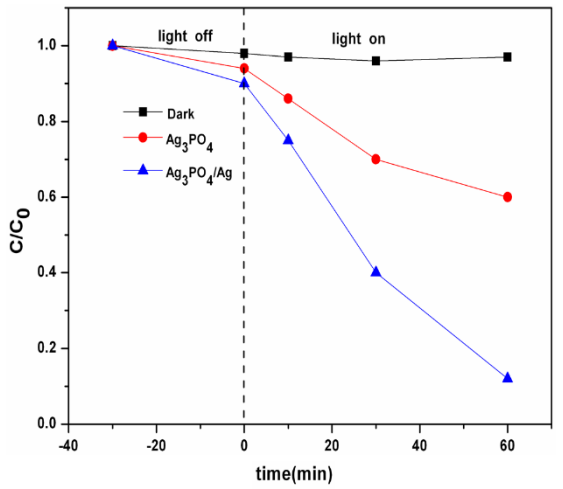

Figure 5. Photocatalytic activities of Ag_3PO_4/Ag composites and pure Ag_3PO_4 particles for RhB degradation under visible-light irradiation (λ> 420 nm).

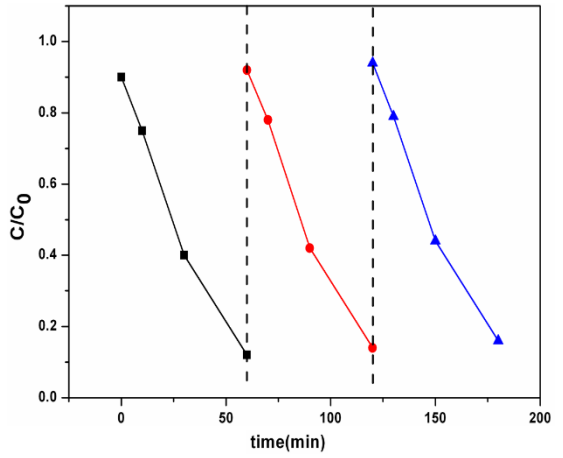

Figure 6. The repeated bleaching of RhB over recycled Ag_3PO_4/Ag photocatalysts under visible light.

stability in the absence of electron acceptors. To elucidate the photocatalytic reaction mechanism, the main species including h^+, $\bullet O^{2-}$ and •OH involved in the photocatalytic process was examined. The method was applied according to the Xiang's report without any modifications[37]. The results indicated that h^+ and $\bullet O^{2-}$ were the main reactive oxidizing species in photocatalytic reaction process of Ag_3PO_4/Ag composites.

Furthermore, to demonstrate the photocatalytic activities of the synthesized Ag_3PO_4/Ag plasmonic photocatalyst for the degradation of distinct organic pollutants, we conducted photocatalytic degradation experiments of RhB, MB and MO. Figure 7a shows the adsorption spectrum of RhB dye over the prepared Ag_3PO_4/Ag photocatalyst. As seen from the observed UV-vis, the absorption peak characteristic of this dye (554 nm) decreases gradually with the increasing of the illumination time. After 90 min irradiation, RhB color was destained by about 98%. The adsorption spectrum of MB in aqueous solution under the same condition is shown in Figure 7b. It indicates that the concentration of MB is decreased as the irradiation time increasing by measuring the intensity of characteristic absorption peak (665 nm), and MB is degraded 78% after 90 min. Finally, discoloration of MO in aqueous solution was tested, by measuring the attenuation of adsorption peak (465 nm) intensity over irradiation time. Again, the color attenuation was observed (Figure 7c), but in a less overall extent (about 40% after 90 min of irradiation) than registered with the previous dyes. Differences in discoloration efficiencies for RhB, MB, and MO dyes can be compared in Figure 7d. The photocatalyst now prepared shows much better performance against cationic dyes (RhB and MB) than to discoloring the anionic dye (MO) solution.

Attempting to clarify that difference, zeta potential measurements for a series of aqueous Ag_3PO_4/Ag suspensions of variable pH values were performed, as shown in Figure 8. The negative values of zeta potential reveal that the as-obtained particles show negative surface charge. Thus, the cationic dye molecules (RhB or MB) could be easily absorbed onto the catalyst surface by electrostatic attraction forces, and charge transfer is facilitated. By contrast, anionic dye molecules (MO) tend to be repulsed and as consequence the action of Ag_3PO_4/Ag plasmonic photocatalyst is less effective.

Based on these results, a possible mechanism is proposed to explain that the enhanced photocatalytic activity and stability of the Ag_3PO_4/Ag plasmonic photocatalyst is due to the synergistic effects between the Ag_3PO_4 nanoparticles and the Ag nanoparticles, as shown in Figure 9. First, the deposition of Ag_3PO_4 nanoparticles on the surface of the Ag nanoparticles can effectively protect Ag_3PO_4 from dissolution, since Ag nanoparticles can retain/store electrons. The photogenerated electrons can be transferred to Ag^0 nanopaticles instead of remaining in Ag_3PO_4 lattice. This will inhibits the reduction of Ag_3PO_4, and then will reduce the molecular oxygen to form the O_2^- active species. Second, The LSPR produced by the collective oscillations of surface electrons on Ag nanoparticles could enhance the local inner electromagnetic field. The electrons generated by the Ag_3PO_4 could be separated efficiency with the help of the local electromagnetic field[34]. Finally, PO_4^{3-} ions own large negative charge and will attract positive holes while repelling

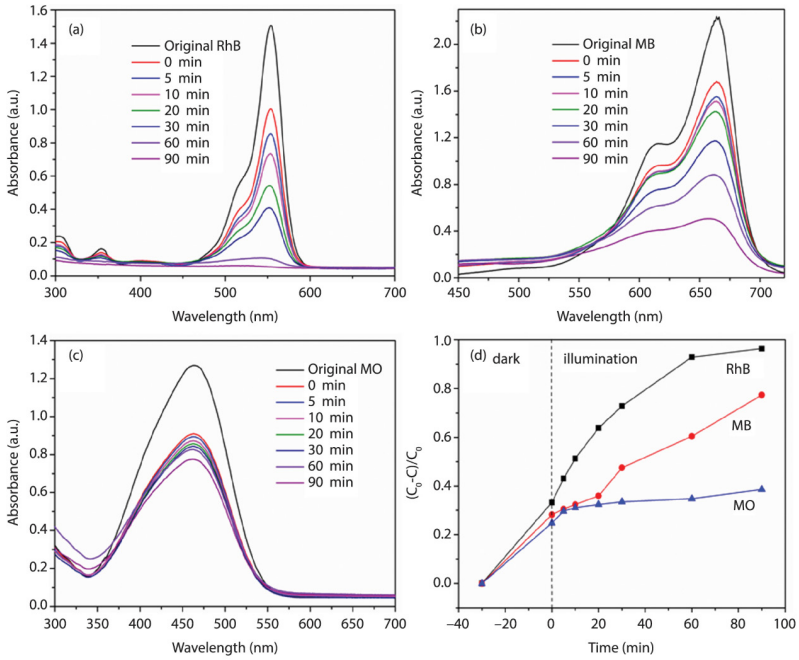

Figure 7. Variations in adsorption spectra of organics dye solution in the presence of the Ag_3PO_4/Ag photocatalyst irradiated under visible light for different time: (a) RhB, (b) MB, (c) MO, and (d) photocatalytic degradation rate of RhB, MB, and MO.

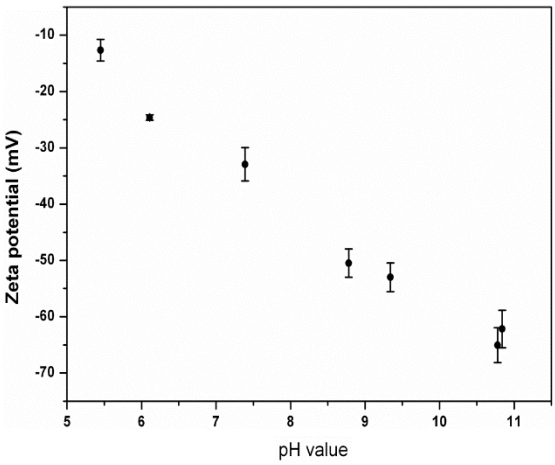

Figure 8. Effect of pH on the zeta potential of Ag_3PO_4/Ag composites in aqueous solution (T= 25 °C).

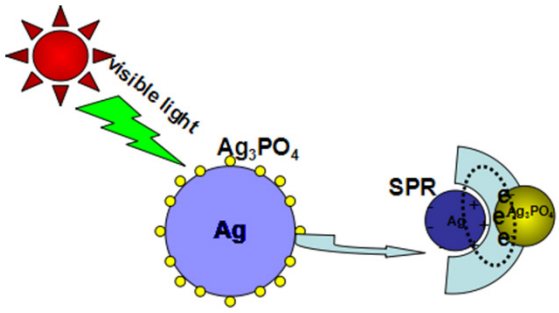

Figure 9. Schematic illustrations of the photocatalytic mechanism of the Ag_3PO_4/Ag photocatalyst.

electrons. Then, photogenerated holes tend to remain on the surface of Ag_3PO_4 nanoparticles. Meanwhile, PO_4^{3-} ions have strong bonding affinity for H_2O molecules. As is well known, H_2O molecules could be easily adsorbed on the surface and then be oxidized by the holes to $OH\cdot$ radicals, being these active apecies to oxidize the dye molecule into carbon dioxide molecules. The above aspects together contributed to the enhanced photocatalytic activity and improved stability of the Ag_3PO_4/Ag plasmonic photocatalyst compared to pure Ag_3PO_4 particles.

4. Conclusions

This work developed a facile approach for the synthesis of Ag_3PO_4/Ag plasmonic photocatalyst. The novel material shows poorer performance in discoloring anionic dye solutions, such as MO dye, in comparison to cationic dyes (RhB and MB). This behavior can be well explained in terms of the exposed negative surface of the Ag_3PO_4/Ag photocatalyst. High efficiency of Ag_3PO_4/Ag photocatalyst arises from LSPR of silver nanoparticles and large negative charge of PO_4^{3-} ions. It is a promising candidate for the removal of hazardous organic materials from wastewater.

Acknowledgements

This research was financially supported by the Natural Science Foundation of Anhui Provincial Education Depart-ment (KJ2015A085), the Natural Science Foundation of Anhui Province (1308085QE73) and the National Natural Science Foundation of China (Nos. 51302002 and 51201002).

References

1. Battiston S, Rigo C, Severo EC, Mazutti MA, Kuhn RC, Gundel A, et al. Synthesis of zinc aluminate ($ZnAl_2O_4$) spinel and its application as photocatalyst. *Materials Research*. 2014; 17(3):734-738. http://dx.doi.org/10.1590/S1516-14392014005000073.
2. Chen X, Shen S, Guo L and Mao SS. Semiconductor-based photocatalytic hydrogen generation. *Chemical Reviews*. 2010; 110(11):6503-6570. http://dx.doi.org/10.1021/cr1001645. PMid:21062099.
3. Linic S, Christopher P and Ingram DB. Plasmonic-metal nanostructures for efficient conversion of solar to chemical energy. *Nature Materials*. 2011; 10(12):911-921. http://dx.doi.org/10.1038/nmat3151. PMid:22109608.
4. Rycenga M, Cobley CM, Zeng J, Li W, Moran CH, Zhang Q, et al. Controlling the synthesis and assembly of silver nanostructures for plasmonic applications. *Chemical Reviews*. 2011; 111(6):3669-3712. http://dx.doi.org/10.1021/cr100275d. PMid:21395318.
5. Thomann I, Pinaud BA, Chen Z, Clemens BM, Jaramillo TF and Brongersma ML. Plasmon enhanced solar-to-fuel energy conversion. *Nano Letters*. 2011; 11(8):3440-3446. http://dx.doi.org/10.1021/nl201908s. PMid:21749077.
6. Awazu K, Fujimaki M, Rockstuhl C, Tominaga J, Murakami H, Ohki Y, et al. A plasmonic photocatalyst consisting of silver nanoparticles embedded in titanium dioxide. *Journal of the American Chemical Society*. 2008; 130(5):1676-1680. http://dx.doi.org/10.1021/ja076503n. PMid:18189392.
7. Tobaldi DM, Pullar RC, Gualtieri AF, Seabra MP and Labrincha JA. Phase composition, crystal structure and microstructure of silver and tungsten doped TiO_2 nanopowders with tuneable photochromic behaviour. *Acta Materialia*. 2013; 61(15):5571-5585. http://dx.doi.org/10.1016/j.actamat.2013.05.041.
8. Tobaldi DM, Pullar RC, Leoni M, Seabra MP and Labrincha JA. Nanosized titania modified with tungsten and silver: microstructural characterisation of a multifunctional material. *Applied Surface Science*. 2013; 287:276-281. http://dx.doi.org/10.1016/j.apsusc.2013.09.141.
9. Chen X, Zhu HY, Zhao JC, Zheng ZF and Gao XP. Visible-light-driven oxidation of organic contaminants in air with gold nanoparticle catalysts on oxide supports. *Angewandte Chemie International Edition*. 2008; 47(29):5353-5356. http://dx.doi.org/10.1002/anie.200800602. PMid:18548470.
10. Han L, Wang P, Zhu C, Zhai Y and Dong S. Facile solvothermal synthesis of cube-like Ag@AgCl: a highly efficient visible light photocatalyst. *Nanoscale*. 2011; 3(7):2931-2935. http://dx.doi.org/10.1039/c1nr10247h. PMid:21611675.
11. Kuai L, Geng B, Chen X, Zhao Y and Luo Y. Facile subsequently light-induced route to highly efficient and stable sunlight-driven Ag-AgBr plasmonic photocatalyst. *Langmuir*. 2010; 26(24):18723-18727. http://dx.doi.org/10.1021/la104022g. PMid:21114257.
12. Hu C, Peng T, Hu X, Nie Y, Zhou X, Qu J, et al. Plasmon-induced photodegradation of toxic pollutants with Ag-AgI/Al_2O_3 under visible-light irradiation. *Journal of the American Chemical Society*. 2010; 132(2):857-862. http://dx.doi.org/10.1021/ja907792d. PMid:20028089.
13. Yi Z, Ye J, Kikugawa N, Kako T, Ouyang S, Stuart-Williams H, et al. An orthophosphate semiconductor with photooxidation properties under visible-light irradiation. *Nature Materials*. 2010; 9(7):559-564. http://dx.doi.org/10.1038/nmat2780. PMid:20526323.
14. Bi Y, Ouyang S, Umezawa N, Cao J and Ye J. Facet effect of single-crystalline Ag_3PO_4 sub-microcrystals on photocatalytic properties. *Journal of the American Chemical Society*. 2011; 133(17):6490-6492. http://dx.doi.org/10.1021/ja2002132. PMid:21486031.
15. Bi Y, Hu H, Ouyang S, Lu G, Cao J and Ye J. Photocatalytic and photoelectric properties of cubic Ag_3PO_4 sub-microcrystals with sharp corners and edges. *Chemical Communications*. 2012; 48(31):3748-3750. http://dx.doi.org/10.1039/c2cc30363a. PMid:22398441.
16. Bi Y, Hu H, Ouyang S, Jiao Z, Lu G and Ye J. Selective growth of Ag_3PO_4 submicro-cubes on Ag nanowires to fabricate necklace-like heterostructures for photocatalytic applications. *Journal of Materials Chemistry*. 2012; 22(30):14847. http://dx.doi.org/10.1039/c2jm32800c.
17. Bi Y, Hu H, Jiao Z, Yu H, Lu G and Ye J. Two-dimensional dendritic Ag_3PO_4 nanostructures and their photocatalytic properties. *Physical Chemistry Chemical Physics*. 2012; 14(42):14486-14488. http://dx.doi.org/10.1039/c2cp42822a. PMid:23032115.
18. Dinh CT, Nguyen TD, Kleitz F and Do TO. Large-scale synthesis of uniform silver orthophosphate colloidal nanocrystals exhibiting high visible light photocatalytic activity. *Chemical Communications*. 2011; 47(27):7797-7799. http://dx.doi.org/10.1039/c1cc12014j. PMid:21633747.
19. Khan A, Qamar M and Muneer M. Synthesis of highly active visible-light-driven colloidal silver orthophosphate. *Chemical Physics Letters*. 2012; 519-520:54-58. http://dx.doi.org/10.1016/j.cplett.2011.11.015.
20. Ge M, Zhu N, Zhao Y, Li J and Liu L. Sunlight-assisted degradation of dye pollutants in Ag_3PO_4 Ssuspension. *Industrial & Engineering Chemistry Research*. 2012; 51(14):5167-5173. http://dx.doi.org/10.1021/ie202864n.
21. Dong P, Wang Y, Li H, Li H, Ma X and Han L. Shape-controllable synthesis and morphology-dependent photocatalytic properties of Ag_3PO_4 crystals. *Journal of Materials Chemistry. A, Materials for Energy and Sustainability*. 2013; 1(15):4651. http://dx.doi.org/10.1039/c3ta00130j.
22. Wang J, Teng F, Chen M, Xu J, Song Y and Zhou X. Facile synthesis of novel Ag_3PO_4 tetrapods and the {110} facets-dominated photocatalytic activity. *CrystEngComm*. 2013; 15(1):39-42. http://dx.doi.org/10.1039/C2CE26060C.
23. Bi Y, Ouyang S, Cao J and Ye J. Facile synthesis of rhombic dodecahedral AgX/Ag_3PO_4 (X = Cl, Br, I) heterocrystals with enhanced photocatalytic properties and stabilities. *Physical Chemistry Chemical Physics*. 2011; 13(21):10071-10075. http://dx.doi.org/10.1039/c1cp20488b. PMid:21519619.
24. Zhang H, Huang H, Ming H, Li H, Zhang L, Liu Y, et al. Carbon quantum dots/Ag_3PO_4 complex photocatalysts with enhanced photocatalytic activity and stability under visible light. *Journal of Materials Chemistry*. 2012; 22(21):10501. http://dx.doi.org/10.1039/c2jm30703k.
25. Liu L, Liu J and Sun DD. Graphene oxide enwrapped Ag_3PO_4 composite: towards a highly efficient and stable visible-light-induced photocatalyst for water purification. *Catalysis Science & Technology*. 2012; 2(12):2525. http://dx.doi.org/10.1039/c2cy20483e.
26. Liang Q, Shi Y, Ma W, Li Z and Yang X. Enhanced photocatalytic activity and structural stability by hybridizing Ag_3PO_4 nanospheres with graphene oxide sheets. *Physical Chemistry Chemical Physics*. 2012; 14(45):15657-15665. http://dx.doi.org/10.1039/c2cp42465g. PMid:23080357.
27. Rawal SB, Sung SD and Lee WI. Novel Ag_3PO_4/TiO_2 composites for efficient decomposition of gaseous 2-propanol under visible-light irradiation. *Catalysis Communications*. 2012; 17:131-135. http://dx.doi.org/10.1016/j.catcom.2011.10.034.

28. Xu YS and Zhang WD. Monodispersed Ag_3PO_4 nanocrystals loaded on the surface of spherical Bi_2MoO_6 with enhanced photocatalytic performance. *Dalton Transactions*. 2013; 42(4):1094-1101. http://dx.doi.org/10.1039/C2DT31634J. PMid:23131725.

29. Zhang L, Zhang H, Huang H, Liu Y and Kang Z. Ag_3PO_4/SnO_2 semiconductor nanocomposites with enhanced photocatalytic activity and stability. *New Journal of Chemistry*. 2012; 36(8):1541. http://dx.doi.org/10.1039/c2nj40206h.

30. Li G and Mao L. Magnetically separable Fe_3O_4-Ag_3PO_4 sub-micrometre composite: facile synthesis, high visible light-driven photocatalytic efficiency, and good recyclability. *RSC Advances*. 2012; 2(12):5108. http://dx.doi.org/10.1039/c2ra20504a.

31. Ma X, Lu B, Li D, Shi R, Pan C and Zhu Y. Origin of Photocatalytic Activation of Silver Orthophosphate from First-Principles. *The Journal of Physical Chemistry C*. 2011; 115(11):4680-4687. http://dx.doi.org/10.1021/jp111167u.

32. Liu JJ, Fu XL, Chen SF and Zhu YF. Electronic structure and optical properties of Ag_3PO_4 photocatalyst calculated by hybrid density functional method. *Applied Physics Letters*. 2011; 99(19):191903. http://dx.doi.org/10.1063/1.3660319.

33. Umezawa N, Shuxin O and Ye J. Theoretical study of high photocatalytic performance of Ag_3PO_4. *Physical Review B: Condensed Matter and Materials Physics*. 2011; 83(3):035202. http://dx.doi.org/10.1103/PhysRevB.83.035202.

34. Liu Y, Fang L, Lu H, Liu L, Wang H and Hu C. Highly efficient and stable Ag/Ag_3PO_4 plasmonic photocatalyst in visible light. *Catalysis Communications*. 2012; 17:200-204. http://dx.doi.org/10.1016/j.catcom.2011.11.001.

35. Liu Y, Fang L, Lu H, Li Y, Hu C and Yu H. One-pot pyridine-assisted synthesis of visible-light-driven photocatalyst Ag/Ag_3PO_4. *Applied Catalysis B: Environmental*. 2012; 115-116:245-252. http://dx.doi.org/10.1016/j.apcatb.2011.12.038.

36. Teng W, Li X, Zhao Q, Zhao J and Zhang D. In situ capture of active species and oxidation mechanism of RhB and MB dyes over sunlight-driven Ag/Ag_3PO_4 plasmonic nanocatalyst. *Applied Catalysis B: Environmental*. 2012; 125:538-545. http://dx.doi.org/10.1016/j.apcatb.2012.05.043.

37. Xiang QJ, Lang D, Shen TT and Liu F. Graphene-modified nanosized Ag_3PO_4 photocatalysts for enhanced visible-light photocatalytic activity and stability. *Applied Catalysis B: Environmental*. 2015; 162:196-203. http://dx.doi.org/10.1016/j.apcatb.2014.06.051.